Assessment of the *GW* approximation using Hubbard chains

Thomas J Pollehn†, Arno Schindlmayr†* and R W Godby‡

† Cavendish Laboratory, University of Cambridge, Madingley Road, Cambridge CB3 0HE, UK

‡ Department of Physics, University of York, Heslington, York YO1 5DD, UK

Abstract

We investigate the performance of the *GW* approximation by comparison to exact results for small model systems. The role of the chemical potentials in Dyson's equation as well as the consequences of numerical resonance broadening are examined, and we show how a proper treatment can improve computational implementations of many-body perturbation theory in general. *GW* and exchange-only calculations are performed over a wide range of fractional band fillings and correlation strengths. We thus identify the physical situations where these schemes are applicable.

1 Introduction

Materials with strong electronic correlation are of considerable interest in solid state science, but their computational treatment is notoriously difficult: diagonalizing the corresponding Hamiltonians is not feasible for large systems, and the strong correlation causes mean-field methods to break down. The collective dynamics of such systems can in principle be described exactly by many-body perturbation theory, however. In this framework, all exchange and correlation effects are absorbed into the self-energy operator Σ, which may be thought of as a non-local, energy-dependent potential. In this paper, we investigate a class of self-energies based on Hedin's *GW* approximation [1]. Their diagrammatic representation, which neglects explicit vertex corrections, is reminiscent of the Fock exchange potential, but the Coulomb interaction includes dynamic screening. Our first aim is to examine whether numerical improvements can be achieved by including further correlation effects in the underlying propagators without

---

*Corresponding author. E-mail address: as10031@phy.cam.ac.uk

changing the diagrammatic form of the self-energy. To assess the performance of these schemes, we compare the calculated spectra with exact results for small model systems that can still be solved by numerical diagonalization techniques. A similar study was recently reported for a two-dimensional Hubbard cluster [2]; here we extend that work by considering further variants as well as a larger variety of systems, most importantly a much wider range of band fillings. Our second aim is to optimize the practical implementation. To this end, we investigate the treatment of the chemical potentials in Dyson's equation and the consequences of resonance broadening in the course of numerical manipulations. Both points are all too often ignored, but may have significant impact on calculated spectra.

The central quantity of interest is the one-particle Green's function G, whose imaginary part is directly linked to the spectral function $A = \pi^{-1}|\operatorname{Im} G|$. While many authors adopt a momentum and energy representation $G(\mathbf{k}, \omega)$ that follows naturally from the band theory of extended systems, we will always consider $G_{\mathbf{RR'}}(\omega)$ in real space, which is more appropriate for finite clusters. Furthermore, this representation has the advantage of showing the entire excitation spectrum in each diagonal element of the Green's function. While this is not always desirable if one wants to concentrate on the evolution of particular quasiparticles, it allows us to judge the performance of any self-energy approximation on the basis of a single matrix element. However, we also calculated G in reciprocal space for corresponding translationally invariant systems to confirm our identification of various spectral features with either quasiparticles or satellites from a particular excitation.

The order of this paper is as follows. Section 2 introduces the model Hamiltonian. In section 3 we describe our procedure for obtaining the exact Green's function. In section 4 we review the GW approximation and address details of the practical implementation. Section 5 lists the approximation variants we consider and gives numerical results. Finally, section 6 contains our conclusions.

2   Model description

The Hubbard model [3] is the classic example of a Hamiltonian that describes strong, short-range electron-electron interaction. It is sufficiently simple to be diagonalized exactly for small cluster sizes using standard numerical techniques, yet its physical behaviour is non-trivial and reflects many properties of real materials. The model variant we employ is a finite chain of M ions with open boundary conditions. Each lattice site contains one orbital that can accommodate up to two electrons with opposite spin. Doubly occupied orbitals are penalized by a repulsive on-site interaction U, while the hopping of transient electrons between neighbouring sites yields an energy gain $-t$. The full Hamiltonian is

$$\mathcal{H} = -t \sum_{\langle \mathbf{R}, \mathbf{R'} \rangle, \sigma} c_{\mathbf{R}\sigma}^{\dagger} c_{\mathbf{R'}\sigma} + U \sum_{\mathbf{R}} \hat{n}_{\mathbf{R}\uparrow} \hat{n}_{\mathbf{R}\downarrow} + \sum_{\mathbf{R}, \sigma} V_{\mathbf{R}} \hat{n}_{\mathbf{R}\sigma} \tag{1}$$
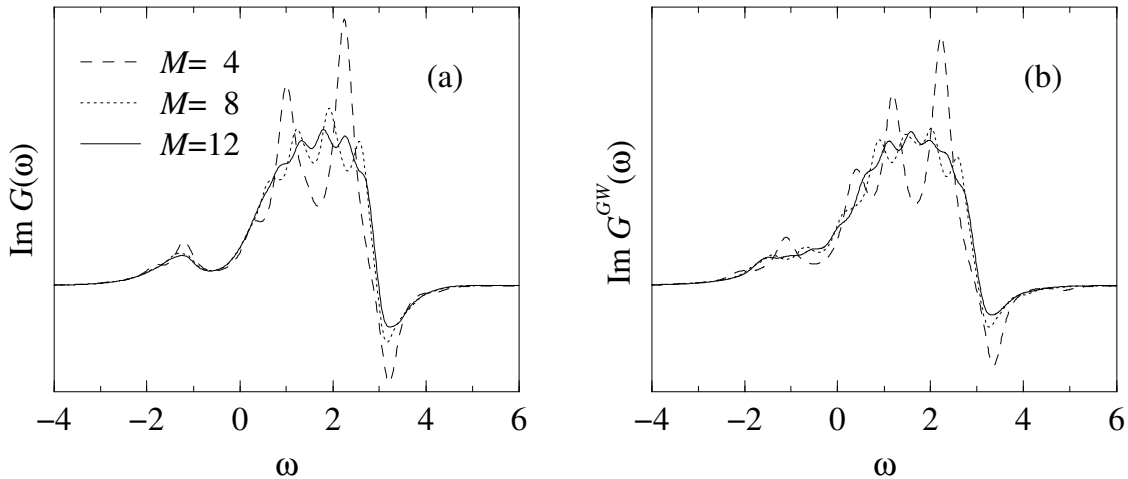
Figure 1: Exact Green's function (a) and GW approximation (b) for varying chain length M with constant 75% band filling and $U = 2$. The broad quasiparticle and satellite spectral features are insensitive to M, indicating that within the Fermi-liquid limitations of the model it is possible to generalize the results reported here.

where $c^\dagger_{\mathbf{R}\sigma}, c_{\mathbf{R}\sigma}$ are the creation and annihilation operators for an electron at site $\mathbf{R}$ with spin σ, $\hat{n}_{\mathbf{R}\sigma} \equiv c^\dagger_{\mathbf{R}\sigma} c_{\mathbf{R}\sigma}$ is the particle number operator, and $\langle \mathbf{R}, \mathbf{R}' \rangle$ indicates a sum over nearest neighbours only. We choose the energy norm by setting $t = 1$. The Hamiltonian further contains a local potential $V_{\mathbf{R}}$ that will later serve as a mean-field approximation for exchange and correlation. We denote the total electron number by N.

The properties of the Hubbard model have been thoroughly investigated. In particular, the one-dimensional case can be solved analytically using the Bethe ansatz [4] and, in the limit of infinite chain length, is known to yield a Luttinger-liquid ground state. The corresponding Green's function describes a gapless spectrum of bosonic collective modes involving charge and spin degrees of freedom [5]. For finite M, however, the renormalized quasiparticle weight factors remain non-zero as long as the Coulomb integral U does not exceed a critical value [6], which behaves asymptotically like $1/M$. In this parameter range the model exhibits Fermi-liquid behaviour. The resolution required to differentiate convincingly between Fermi liquids and Luttinger liquids is in fact near infinitesimal on the energy scale we consider, and the Lorentzian broadening of resonances essentially wipes out features on a genuinely small scale that are of primary concern in the distinction between the two. Even so, we have confirmed that all systems we study in this paper are comfortably within the Fermi-liquid regime, so that the same perturbation methods as for higher dimensions can be applied.

As we are working with small model Hamiltonians, it is essential to consider the possible sensitivity of our results to the parameters in (1). The system size is a particularly important aspect. We have calculated the exact Green's function and a correponding GW approximation for varying chain length while keeping $U = 2$ and the fractional band filling $N/(2M) = 75\%$ constant. In figure 1, as in all later graphs, we show the

matrix element $\operatorname{Im} G_{1,1}(\omega)$ in arbitrary units and align the chemical potentials to facil-iate comparison. The number of peaks in the spectral function grows with the chain length as expected. However, it is also evident that the *qualitative* appearance of the graphs changes little: the broad quasiparticle and satellite peaks are insensitive to M. This becomes even clearer when the integral $\int_{-\infty}^{\omega} \operatorname{Im} G(\omega') \, d\omega'$, which averages over os-cillations on a small scale, is considered. We have thus demonstrated that the results reported in the following sections are relatively insensitive to the chain length and so retain significance beyond the particular model geometry, although of course the for-mal extrapolation to $M \to \infty$ cannot be made because of the eventual transition to a Luttinger liquid.

3   Exact numerical solution

The exact one-particle Green's function at zero temperature is defined as

$$G_{\mathbf{R}\mathbf{R}'}(t - t') = -\mathrm{i}\langle N|\mathcal{T}\{c_{\mathbf{R}\sigma}(t)c_{\mathbf{R}'\sigma}^{\dagger}(t')\}|N\rangle \tag{2}$$

where $|N\rangle$ is the ground state of the interacting N-electron system, $\mathcal{T}$ is Wick's time-ordering operator, and $c_{\mathbf{R}\sigma}(t) \equiv \exp(\mathrm{i}\mathcal{H}t)c_{\mathbf{R}\sigma}\exp(-\mathrm{i}\mathcal{H}t)$ denotes the time-dependent wave field operator in the Heisenberg picture. We have suppressed the spin index in G because the Green's function is diagonal and degenerate in σ. It is convenient to Fourier transform (2) to the energy domain and rewrite the Green's function in the form

$$G_{\mathbf{R}\mathbf{R}'}(\omega) = \langle N|c_{\mathbf{R}\sigma}\frac{1}{\omega - \mathcal{H}^{+} + E_N}c_{\mathbf{R}'\sigma}^{\dagger}|N\rangle + \langle N|c_{\mathbf{R}'\sigma}^{\dagger}\frac{1}{\omega + \mathcal{H}^{-} - E_N}c_{\mathbf{R}\sigma}|N\rangle. \tag{3}$$

Here E_N is the ground-state energy corresponding to $|N\rangle$ and $\mathcal{H}^{\pm}$ denotes the Hamil-tonian matrix for $N \pm 1$ electrons.

The main computational difficulty is that the number of basis vectors of the many-body problem grows exponentially with the system size, because it quantifies the $(2M!)$ $/[(2M-N)!N!]$ possibilities of distributing N electrons onto M two-fold spin-degenerate orbitals. For a ten-site chain at half filling, the largest model we consider, this implies a basis size of 184,756 (although greater chain lengths are feasible if the band filling is very small or very large). However, less than 0.01% of the elements of $\mathcal{H}$ are non-zero, so that sparse-matrix techniques may be used to obtain $|N\rangle$ and E_N.

The diagonal elements $G_{\mathbf{R}\mathbf{R}}$, which enter the calculation of the electron density and other quantities, may be calculated without full matrix inversion by tridiagonalizing $\omega \mp \mathcal{H}^{\pm} \pm E_N$ using the recursion method [7] and starting with the vector $c_{\mathbf{R}'\sigma}^{\dagger}|N\rangle$ or $c_{\mathbf{R}\sigma}|N\rangle$. For non-diagonal elements a block recursion must be performed. Neither an inversion nor a complete diagonalization would be feasible in terms of computer memory: for the example $M = N = 10$ mentioned above, 210 GB are required to store the eigenvectors of $\mathcal{H}^{\pm}$ and 254 GB for the inverse of $\omega \mp \mathcal{H}^{\pm} \pm E_N$, although this could be somewhat reduced by exploiting symmetry relations.

Once the recursion coefficients, i.e., the diagonal elements a_n and the off-diagonal elements b_n^2 of the tridiagonal matrix, are determined iteratively up to a suitable recursion depth D, the elements of the Green's function are obtained from

$$G_{\mathbf{RR}}(\omega) = \cfrac{1}{\omega - a_0 - \cfrac{b_1^2}{\omega - a_1 - \cdots - \cfrac{b_D^2}{\omega - a_D}}}. \tag{4}$$

Even with a basis size of 184,756 about 400 recursions are sufficient, since the number of actual spectral features is small compared to the basis size. Ideally a single recursive level for each additional peak in the spectrum would be necessary, and indeed we require only a few recursions per feature to achieve full convergence in practice. The quasiparticles and collective excitations of the N-electron system are determined by the eigenvalues of $\mathcal{H}^\pm$ and feature as simple poles in the Green's function. For numerical convenience, we broaden these sharp resonances into Lorentzians by offsetting the singularities from the real energy axis by a distance δ. This procedure does not imply a finite lifetime of the excited states.

4 The GW approximation

The GW approximation constitutes a diagrammatic expansion of the self-energy that neglects explicit vertex corrections. However, it includes dynamic screening of the Coulomb interaction and is thus capable of describing certain correlation effects. Originally the GW self-energy was derived as a first order iterative solution of Hedin's coupled equations for the propagators of the interacting many-electron system starting from Hartree theory [1]. In this section we briefly review the formalism and subsequently address crucial details concerning the computational implementation.

4.1 The self-energy in the GW approximation

Starting from a mean-field Hamiltonian that may contain a suitable effective potential V, we obtain a zeroth order Green's function

$$G_{\mathbf{RR}'}^0(\omega) = \sum_s \frac{\langle \mathbf{R}|\psi_s\rangle\langle\psi_s|\mathbf{R}'\rangle}{\omega - \epsilon_s + \mathrm{i}\,\mathrm{sgn}(\epsilon_s - \mu_0)\delta} \tag{5}$$

in terms of the one-particle eigenstates $|\psi_s\rangle$ and corresponding energy eigenvalues ϵ_s. The symbol μ_0 denotes the chemical potential. Conventionally, the random phase approximation

$$P_{\mathbf{RR}'}^{\mathrm{RPA}}(\tau) = -2\mathrm{i}G_{\mathbf{RR}'}^0(\tau)G_{\mathbf{R}'\mathbf{R}}^0(-\tau) \tag{6}$$

for the irreducible polarization propagator is employed, with $\tau \equiv t - t'$ and a factor 2 for spin summation. The dynamically screened interaction is then obtained from

$$W^{\text{RPA}}(\omega) = U \left[1 - P^{\text{RPA}}(\omega)U \right]^{-1} \tag{7}$$

in matrix notation. Finally, the self-energy is given by the expression

$$\Sigma^{GW}_{\mathbf{R}\mathbf{R}'}(\tau) = \mathrm{i} G^0_{\mathbf{R}\mathbf{R}'}(\tau) W^{\text{RPA}}_{\mathbf{R}\mathbf{R}'}(\tau + \eta) \tag{8}$$

to which the GW approximation owes its name. η denotes a positive infinitesimal. The self-energy may be inserted into Dyson's equation to yield the improved Green's function

$$G^{GW}(\omega) = \left[1 - G^0(\omega) \left(V^{\text{H}} + \Sigma^{GW}(\omega) - V \right) \right]^{-1} G^0(\omega) \tag{9}$$

where $V^{\text{H}}_{\mathbf{R}} = U\langle \hat{n}_{\mathbf{R}\uparrow} + \hat{n}_{\mathbf{R}\downarrow} \rangle$ indicates the Hartree potential. During the calculation we use Fast Fourier Transforms to change between the time and energy domains as appropriate in order to avoid costly numerical convolutions.

4.2   Alignment of the chemical potentials

Dyson's equation (9) combines the equation of motion of the interacting with that of the corresponding non-interacting system. The self-energy specifies the deviation of the quasiparticle states from the bare electrons and holes upon adiabatic introduction of the Coulomb potential. It is thus an equilibrium quantity that should really be calculated self-consistently, i.e., the dressed Green's function obtained from Dyson's equation is reinserted into the self-energy until convergence has been achieved. This procedure is so computationally demanding, however, as to make it unfeasible for large-scale *ab initio* calculations. Furthermore, while the random phase approximation $P^{\text{RPA}}[G^0]$ by construction gives the proper response function of time-dependent Hartree theory, the same expression evaluated with a self-consistent Green's function ceases to yield a physically meaningful propagator due to the neglect of appropriate vertex corrections. As a consequence the spectrum becomes broad and structureless [8]. On the other hand, the self-energy inherits the chemical potential of the underlying Green's function, and a mismatch with that of the dressed propagator may result in wrong time-ordering.

A possible solution is to use a zeroth order G^0 to evaluate the self-energy but shift it in such a way as to align its chemical potential with that of the dressed Green's function. This limited degree of self-consistency, originally suggested by Hedin [1], suffices to ensure the correct time-ordering while leaving the response function unchanged and thus physically meaningful. From the Fourier transform of (8), we see that shifting G^0 by an amount $\tilde{\omega}$ on the energy axis translates into an identical shift of the self-energy

$$\Sigma^{GW}_{\mathbf{R}\mathbf{R}'}(\omega - \tilde{\omega}) = \frac{\mathrm{i}}{2\pi} \int G^0_{\mathbf{R}\mathbf{R}'}(\omega - \tilde{\omega} - \omega') W^{\text{RPA}}_{\mathbf{R}\mathbf{R}'}(\omega') \mathrm{e}^{\mathrm{i}\eta\omega'} \, \mathrm{d}\omega' \tag{10}$$

where the contour is closed about the upper half-plane. According to Dyson's equation, the chemical potential of the dressed Green's function becomes $\mu = \mu_0 + \langle V^{\text{H}} + \Sigma^{GW}(\mu -$
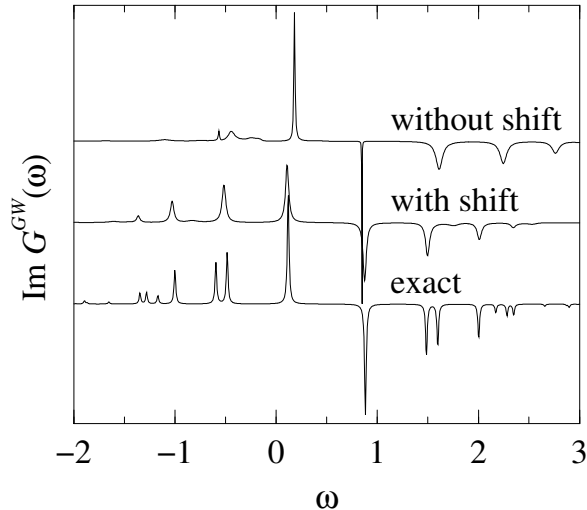
Figure 2: The self-consistency shift $\tilde{\omega}$, which aligns the chemical potential of the zeroth order G^0 with that of the dressed Green's function derived from it, improves the spectral features substantially even for a very weak interaction of $U = 1$. The exact spectrum is shown for comparison.

$\tilde{\omega}) - V\rangle$, where the matrix element is to be taken with the highest occupied quasiparticle orbital. In practice we use the corresponding $|\psi_s\rangle$ of the non-interacting system. The shift is determined so that the chemical potential coincides exactly with that of the relocated zeroth order Green's function, hence $\mu = \mu_0 + \tilde{\omega}$. Inserting this relation into the previous equation yields the explicit solution

$$\tilde{\omega} = \langle V^{\mathrm{H}} + \Sigma^{GW}(\mu_0) - V\rangle. \tag{11}$$

Despite its early suggestion, this self-consistency shift is often ignored in *ab initio* band structure calculations, where its impact is normally small. It may substantially improve the more sensitive satellite spectrum, however. As an example we consider an eight-site chain at half-filling with $U = 1$. In figure 2 we display results obtained with and without $\tilde{\omega}$. The exact spectrum is shown for comparison. While the shift has little effect on the quasiparticle peaks, the improved description of the satellites is evident even for such a weak interaction. The results follow our previous demonstration that to a large extent $\tilde{\omega}$ also restores particle number conservation, which is generally violated in non-self-consistent many-body theory [9]. All subsequent calculations incorporate $\tilde{\omega}$.

4.3 Infinitesimal peak broadening

The *GW* approximation constitutes a diagrammatic expansion of the true self-energy to first order in the screened interaction. The underlying equations (6) to (9) may be solved in the time as well as in the energy domain. While we employ Fast Fourier Transforms to switch between the two as appropriate, most implementations work exclusively in
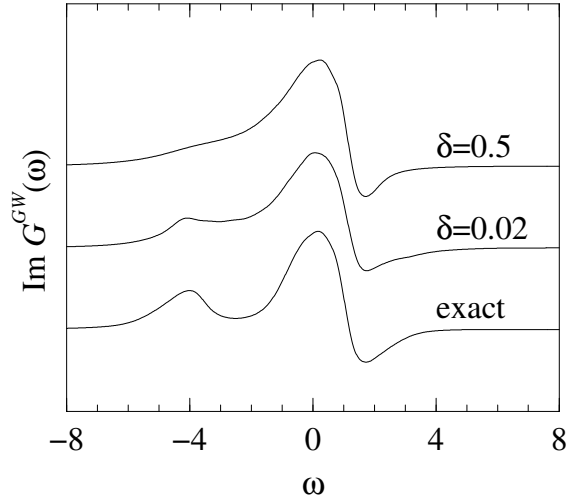
Figure 3: Comparison of spectra calculated with $\delta = 0.5$ and $\delta = 0.02$, where the latter was broadened afterwards. The smaller Lorentzian width incurs a higher computational cost but yields more pronounced spectral features.

the latter, where all operations are either multiplicative or feasible but computationally costly convolutions. It is frequently ignored, however, that the relations are only strictly valid in the limit $\delta \to 0$, because convolutions with a finite displacement of the singularities from the energy axis will mix the real and imaginary parts of the propagators. As a consequence, weak features such as satellites tend to smear out and may even become undetectable in the calculated spectrum. As an example, figure 3 contrasts the spectral functions from two calculations with $\delta = 0.5$ and $\delta = 0.02$, where the resonances in the latter were suitably broadened afterwards for the purpose of comparison. We also show the exact spectrum. The model specifications are $M = 10$, $N = 14$ and medium interaction $U = 4$. The features in the second curve are clearly more pronounced. In particular, the reproduction of the satellite at -4 is superior. The downside of using small values for δ is an increased number of sampling points, because the energy resolution in a numerical treatment must necessarily exceed the characteristic peak width. In the following we always choose δ as small as computationally possible and only broaden the final spectra to achieve a Lorentzian width of 0.5 for visualization.

5   Comparison of different approximation variants

In this section we investigate in detail several variants of the GW scheme by direct comparison with exact results. The main criterion we apply to judge approximations is their ability to reproduce the overall shape of the true spectral function, i.e., the position and weight of the quasiparticle excitations as well as their satellites.

5.1   Different initial Hamiltonians

The framework outlined in section 4 allows for considerable freedom in the choice of the initial mean-field Hamiltonian. We here consider the following options in order of increasing complexity.

1. Hedin's original iterative derivation suggests that the Hartree approximation $V = V^{\mathrm{H}}$ with self-consistently determined site occupation numbers should be used, although this is rarely done in practice.

2. The most common choice in *ab initio* calculations is to start with a self-consistent exchange-correlation potential from density-functional (DF) theory, which yields the same charge density as the interacting system. We simulate this procedure by numerically determining a potential $V = V^{\mathrm{H}} + V^{\mathrm{xc}}$ that reproduces the occupation numbers $\langle \hat{n}_{\mathbf{R}\sigma} \rangle$ of the exact solution. We still refer to this approach as density-functional theory, although it is really a *site occupation function(al) theory* [10].

3. We can also evaluate the self-energy (8) with the exact Green's function G, which is fully renormalized and contains a background satellite spectrum. While this approach itself is of course not directly relevant to practical calculations, it serves as an example for implementations that attempt to include a maximum amount of many-body features in the initial Green's function.

It was long regarded as self-evident that including as much information about exchange and correlation as possible in the initial zeroth order Hamiltonian will provide an optimal starting point for the iteration. Since the extra computational cost required to include a Hartree or local-density mean-field in the Hamiltonian is negligible compared to a complete GW calculation, this approach possesses great appeal. As our model is numerically solvable, we are in fact able to use the exact Green's function as an extreme example of an improved propagator that tries to incorporate as many correlation effects as possible up to dynamic renormalization. Besides the conventional random phase approximation $W^{\mathrm{RPA}}[G^0]$ with density-functional theory as a zeroth order approximation we have evaluated the same diagrams using the exact Green's function to obtain the more sophisticated $W^{\mathrm{RPA}}[G]$, which contains a rich satellite spectrum. Note, however, that this is not the exact screening, since vertex corrections in the polarization are still ignored. In figure 4 we show the exact spectrum together with the results from the four possible combinations of these dielectric functions with G^0 and G in the self-energy for two electrons on a twelve-site chain with $U = 2$. Evidently the four curves differ very little, implying that renormalization does not improve the spectrum, but the computational expense is considerably higher if the exact Green's function is used either in the screening or the self-energy.

   The rule emerging here is that there is no particular advantage in sophisticated, renormalized propagators when one works within the GW scheme. Instead these should be *consistent* with the current level of iteration, because the self-energy (8) neglects
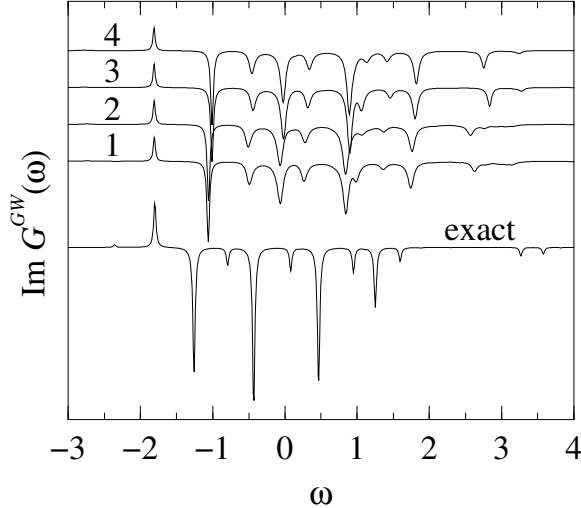
Figure 4: Using a renormalized Green's function or screening in the GW self-energy without vertex corrections fails to improve the spectrum. The numbered curves indicate the combinations (1) $G^0W^{\mathrm{RPA}}[G^0]$, (2) $GW^{\mathrm{RPA}}[G^0]$, (3) $G^0W^{\mathrm{RPA}}[G]$ and (4) $GW^{\mathrm{RPA}}[G]$ for two electrons on a twelve-site chain with $U = 2$.

explicit vertex corrections and so does not become exact when evaluated using the true propagators. In general, overrealistic propagators may even cause the approximation to deteriorate, because they destroy the balance that exists between the internal diagrammatic expansion of the Green's function and screening on the one hand and the vertex function on the other [11]. We thus restrict ourselves to Hartree and density-functional theory as zeroth order approximations in the following and present results for these cases below.

5.2   Model dielectric functions

As the random phase approximation demands inconvenient numerical convolutions in the energy domain, practical implementations frequently deviate from the original GW scheme by employing alternative model dielectric functions that can be evaluated directly [12]. In order of increasing complexity, the following options present themselves.

1. Neglecting screening effects and using the bare Coulomb interaction is particularly inexpensive, because no intermediate polarization propagator is required. In this case the self-energy

$$\Sigma^{\mathrm{x}}_{\mathbf{R}\mathbf{R}'} = -U\langle \hat{n}_{\mathbf{R}\sigma} \rangle \delta_{\mathbf{R}\mathbf{R}'} \tag{12}$$

is diagonal and energy-independent. We denote the corresponding Green's function, which contains electronic exchange but no dynamic correlation, by G^{x}. If

performed self-consistently, this approach is identical to the Hartree–Fock treatment.

2. The screening $W^{\mathrm{RPA}}[G^0]$ may be calculated in the random phase approximation from the zeroth order Green's function in accordance with the original proposition of the GW approximation, yielding G^{GW}.

3. Irrespective of the initial mean-field Hamiltonian, we can employ a realistic screened interaction that contains more correlation effects. However, we have already argued earlier that a unilateral expansion of the screened interaction will not improve the spectrum, and figure 4 gave a numerical example with $W^{\mathrm{RPA}}[G]$ to this effect. Therefore we will not consider this option further.

In figure 5 we show the exact spectral function for a ten-site chain together with four approximations, namely G^{GW} and G^{x} evaluated both with Hartree and density-functional theory as zeroth order Hamiltonians. We increase the band filling from 50% in two steps to 90% and consider the situation of medium ($U = 4$) as well as strong ($U = 8$) correlation. Due to the particle-hole symmetry of the Hubbard model, the spectrum for band fillings below 50% can be obtained by inflection. For reference, we quote the effective potential parameters $V_{\mathbf{R}}$ for a selected system with 70% band filling and $U = 4$ in table 1.

Irrespective of the correlation strength, the occupation numbers are necessarily uniform at half filling due to particle-hole symmetry. Hence in this case the dressed Green's functions derived from Hartree and density-functional theory as starting points coincide except for a constant shift. The exchange Σ^{x} is also uniform and causes just another constant shift, while the GW approximation improves slightly but still fails to reproduce the true spectrum satisfactorily, especially for large U. For instance, the energy gap in figure 5(b) is crucially underestimated. On the plus side, the approximations have the correct symmetry about the chemical potential. As the band filling increases, the GW approximation at first becomes better but again deteriorates for very large band filling. The dominant interaction processes in this limit are described by the T-matrix [13], which renormalizes the Hartree–Fock potential by including multiple scattering in the particle-particle channel to all orders. Σ^{GW} ignores these diagrams and so does not reproduce the spectrum well: it is outperformed even by the unrenormalized exchange approximation. The GW approximation works best for intermediate band filling as in figures 5(c) and (d), where it yields good results even for strong correlation. In this regime there is also little difference between Hartree and density-functional theory as starting points, unlike for higher band filling where the GW approximation breaks down. The description of quasiparticles is in general superior to that of satellites, which are more sensitive to the specific form of many-body interaction processes. The bare exchange approximation naturally works best in situations where screening effects are negligible, i.e., if the interaction is weak and/or the band filling is very high, such as in figure 5(e). The absence of long-range interaction in the Hubbard model adds to this effect. Hartree theory as a zeroth order approximation gives consistently better results
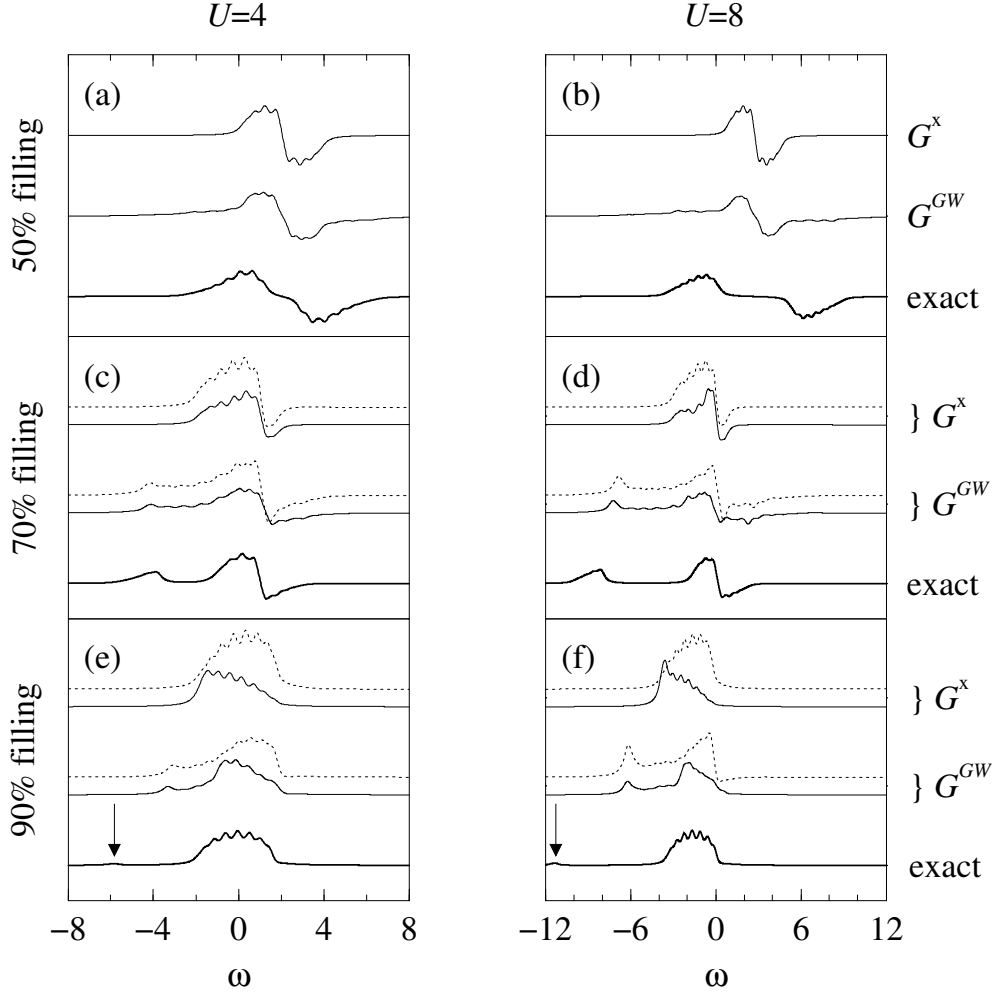
Figure 5: The exact Green's function for a ten-site chain compared to the GW approximation G^{GW} and the exchange-only G^x for different band fillings $N/(2M)$ and correlation strengths U. Where pairs of curves are shown, the solid line refers to a zeroth order density-functional and the dotted line to a Hartree Hamiltonian. Some small satellites are marked by arrows. The GW scheme performs best for intermediate band filling. The exchange-only scheme yields increasingly accurate quasiparticles for high band filling and weak correlation but cannot produce satellites.

Table 1: Effective potential parameters in Hartree and density-functional (DF) theory for ten sites with 70% band filling and $U = 4$. The chain is symmetric about its centre.

Site index	1;10	2;9	3;8	4;7	5;6
Hartree	0.26	−0.02	0.06	0.10	0.06
DF	0.26	−0.33	−0.08	−0.06	−0.15

than density-functional theory. Being an effective mean field, Σ^{x} of course cannot produce a satellite structure. This is acceptable, however, because collective excitations carry little spectral weight in the limits of small U and high fractional band filling.

6 Conclusions

We have examined the implementation and performance of the GW approximation by comparing exact and approximate spectra for finite Hubbard chains that exhibit Fermi-liquid behaviour. The insensitivity with respect to the chain length makes the results transferable, although further investigations for higher-dimensional systems will be useful. Focusing on the computational implementation, we pointed out that the mathematical structure of many-body perturbation theory requires a shift aligning the chemical potentials in Dyson's equation as well as a minimization of the artificial Lorentzian broadening of spectral peaks. In each case model calculations clearly demonstrated improvements in the GW approximation, particularly with respect to the satellite spectrum. Next we studied the performance of the GW and the related bare exchange approximation for various band fillings and correlation strengths. Our results show that the former can yield good results for intermediate band filling even if the correlation is strong, while the latter provides a computationally cheaper alternative for weak correlation and small or high band filling. The description of quasiparticles is generally better than that of satellites. We have also shown evidence that renormalized propagators will not improve the GW approximation without the inclusion of appropriate vertex corrections in the self-energy.

Acknowledgments

References

[1] Hedin L 1965 *Phys. Rev.* **139** A796

[2] Verdozzi C, Godby R W and Holloway S 1995 *Phys. Rev. Lett.* **74** 2327

[3] Hubbard J 1963 *Proc. R. Soc.* **276** 238

[4] Lieb E H and Wu F Y 1968 *Phys. Rev. Lett.* **20** 1445

[5] Meden V and Schönhammer K 1992 *Phys. Rev.* B **46** 15 753

   Voit J 1993 *Phys. Rev.* B **47** 6740; 1993 *J. Phys.: Condens. Matter* **5** 8305

[6] Qin S, Qian T, Yu L and Su Z 1995 *Phys. Rev.* B **51** 16 594

[7] Haydock R 1980 *Solid State Physics* vol 35, ed H Ehrenreich *et al* (New York: Academic) p 216

[8] von Barth U and Holm B 1996 *Phys. Rev.* B **54** 8411

[9] Schindlmayr A 1997 *Phys. Rev.* B **56** 3528, cond-mat/9709275

[10] Schindlmayr A and Godby R W 1995 *Phys. Rev.* B **51** 10 427, cond-mat/9709266

   Schönhammer K, Gunnarsson O and Noack R M 1995 *Phys. Rev.* B **52** 2504

[11] de Groot H J, Bobbert P A and van Haeringen W 1995 *Phys. Rev.* B **52** 11 000

   Shirley E L 1996 *Phys. Rev.* B **54** 7758

[12] Engel G E and Farid B 1993 *Phys. Rev.* B **47** 15 931

[13] Galitskii V 1958 *Sov. Phys.–JETP* **7** 104